Molecular Structure, Bonding, and Jahn−Teller Effect in Gold Chlorides: Quantum Chemical Study of $AuCl_3$, Au_2Cl_6, $AuCl_4^-$, AuCl, and Au_2Cl_2 and Electron Diffraction Study of Au_2Cl_6

Magdolna Hargittai,*,† Axel Schulz,*,‡ Balázs Réffy,† and Mária Kolonits†

Contribution from the Structural Chemistry Research Group of the Hungarian Academy of Sciences, Eötvös University, Pf. 32, H-1518 Budapest, Hungary and the Institute of Inorganic Chemistry, LMU−University of Munich, Butenandtstrasse 5−13 (Haus D), D-81377 Munich, Germany

Received August 15, 2000

Abstract: The molecular geometry of dimeric gold trichloride has been determined by gas-phase electron diffraction and high-level quantum chemical calculations. The molecule has a planar, D_{2h}-symmetry halogen-bridged geometry, with the gold atom in an almost square-planar coordination. The geometrical parameters from electron diffraction (r_g and $\angle_\alpha$) are: Au−Cl_t, 2.236 ± 0.013 Å; Au−Cl_b, 2.355 ± 0.013 Å; $\angle Cl_t$−Au−Cl_t, 92.7 ± 2.5°; and $\angle Cl_b$−Au−Cl_b, 86.8 ± 1.8° (t, terminal; b, bridging chlorine). Quantum chemical calculations have also been carried out on the ground-state and transition-state structures of monomeric $AuCl_3$; both have C_{2v}-symmetry structures due to Jahn−Teller distortion. CASSCF calculations show that the triplet D_{3h}-symmetry structure lies ∼29 kcal/mol above the $^1A_1$ symmetry ground state. The Mexican-hat-type potential energy surface of the monomer has three equal minimum-energy positions around the brim of the hat, separated by three transition-state structures, ∼6 kcal/mol higher in energy, at the CASSCF level. The distortion of $AuCl_3$ is smaller than that of AuF_3, and the possible reasons are discussed. The structure of the $AuCl_4^-$ ion has also been calculated, the latter both in planar, D_{4h}, and tetrahedral, T_d, arrangements. The tetrahedral configuration of $AuCl_4^-$ is subject to Jahn−Teller effect, which leads to a complicated potential energy surface. The factors leading to the planar geometry of $AuCl_4^-$ and Au_2Cl_6 are discussed. The frequently suggested dsp^2 hybridization as a possible cause for planarity is not supported by this study. The geometries of AuCl and Au_2Cl_2 have also been calculated. The very short Au···Au distance in the latter, similarly to Au_2F_2, is indicative of the aurophilic interaction.

Introduction

The structures of gold halides, especially those of the trihalides, differ from the structures of most other metal trihalides. Gold trifluoride forms a helix in the crystal[1] and planar dimeric molecules in the low-temperature gas phase;[2] and Jahn−Teller-distorted monomeric molecules are present at higher temperatures.[2] These experimental findings have been confirmed by ab initio calculations.[2,3] The crystal of gold trichloride consists of planar dimeric units,[3,4] similarly to those found in the low-temperature gas of gold trifluoride. The gas-phase structure of the molecule has not been determined experimentally, but an earlier Hartree−Fock calculation indicated geometries similar to those of the trifluoride.[3]

Structural studies of gold halides are demanding exercises, both experimentally and computationally.[2,3,5−8] Their gas-phase study requires special experimental conditions,[2] and their computations are difficult, due to the size of the gold atom. Most computations so far have been concerned with the monohalides of gold and its trifluoride. We found it of interest to determine the structure of gas-phase gold trichloride by electron diffraction experiment and augment it with high-level computations. We also intended to investigate the reason for planarity in the gold halide dimers, and in this connection we also calculated the structure of the $AuCl_4^-$ ion, known to be similarly square planar, rather than tetrahedral.[3,9]

The Jahn−Teller effect[10] is a somewhat elusive phenomenon in structural chemistry that is observed in the crystal phase more frequently than in the gas phase. More often than not, there is only a strong indication rather than unambiguous evidence of its manifestation in molecules through small geometrical distortions or enlarged vibrational amplitudes. This is especially the case with molecules in which the central atom has a d^1 electronic

* To whom correspondence should be addressed. E-mail: hargittaim@ludens.elte.hu; lex@cup.uni-muenchen.de.

† Eötvös University.

‡ University of Munich.

(1) (a) Einstein, F. W. B.; Rao, P. R.; Trotter, J.; Bartlett, N. *J. Chem. Soc.* (*A*) **1967**, 478. (b) Zemva, B.; Lutar, K.; Jesih, A.; Casteel, W. J.; Wilkonson, A. P.; Cox, D. E.; Von Dreele, R. B.; Borrmann, H.; Bartlett, N. *J. Am. Chem. Soc*. **1991**, *113*, 4192.

(2) Réffy, B.; Kolonits, M.; Schulz, A.; Klapötke, T. M.; Hargittai, M. *J. Am. Chem. Soc*. **2000**, *122*, 3127.

(3) Schwerdtfeger, P.; Boyd, P. D. W.; Brienne, S.; Burrell, A. K. *Inorg. Chem*. **1992**, *31*, 3411.

(4) Clark, E. S.; Templeton, D. H.; MacGillavry, C. H. *Acta Crystallogr*. **1958**, *11*, 284.

(5) Schwerdtfeger, P.; McFeaters, J. S.; Liddell, M. J.; Hrusak, J.; Schwarz, H. *J. Chem. Phys*. **1995**, *103*, 245.

(6) Schwerdtfeger, P. *Mol. Phys*. **1995**, *86*, 359.

(7) Schröder, D.; Hrusák, J.; Tornieporth-Oetting, I. C.; Klapötke, T. M.; Schwarz, H. *Angew. Chem*. **1994**, *106*, 223.

(8) Hector, A. L.; Levason, W.; Weller, M. T.; Hope, E. G. J. *J. Fluorine Chem*. **1997**, *86*, 105.

(9) (a) Jones, P. G. *Gold Bull*. **1981**, *14*, 159. (b) Raubenheimer, H. G.; Cronje, S. In *Gold*: *Progress in Chemistry, Biochemistry and Technology*; Schmidbaur, H. Ed.; John Wiley & Sons: Chichester, 1999; pp 588−623.

(10) Jahn, H. A.; Teller, E. *Proc. R. Soc., London, Ser. A* **1937**, *161*, 220.

10.1021/ja003038k CCC: $20.00
Published on Web 01/24/2001

configuration, for which only a relatively small distortion can be expected.[11,12] The largest distortions are to be found in d^4 systems with octahedral, and for d^8 systems with tetrahedral, coordination. Similarly large distortions occur in D_{3h}-symmetry trihalides of metals with both d^4 and d^8 electronic configuration, as the gas-phase structure of MnF_3 (d^4)[13] and AuF_3 (d^8)[2] illustrate. In both cases, the peak on the radial distribution curve, from electron diffraction, corresponding to the F···F nonbonded interaction splits into two, thus providing direct evidence of the strong distortion. The possibility of the distortion in three-coordinated gold complexes had been suggested on the basis of simple Hückel-type calculations.[14] We wanted to investigate the extent of the Jahn−Teller effect in $AuCl_3$, for which its presence has already been indicated,[3] and also look at the potential energy surface of $AuCl_4^-$, which is expected to be especially complicated by the multidimensional distortion space with many possible lower symmetry structures due to the doubly and triply degenerate *e*- and t_2-type Jahn−Teller active vibrations.

Experimental Section

The electron diffraction patterns of a Sigma−Aldrich gold trichloride sample (99.99+% purity) were recorded in our modified EG-100A apparatus[15] with a nickel nozzle system.[16] The sample appeared to be extremely sensitive to heating. To facilitate stabilization of the experimental conditions, the nozzle was passivated for 36 h at 100 °C under 100 atm Cl_2 gas prior to the diffraction experiment. The first attempt at 490 K gave changing diffraction patterns at repeated runs, indicating decomposition of the sample. We succeeded in eliminating this problem by lowering the temperature to ∼460 K and using longer exposures. Even with these precautions, there was a residue left in the nozzle, which proved to be pure gold. We suspected that the partial decomposition of the dimer to elementary materials took place during the heating, rather than the cooling, of the sample. Indeed, our subsequent analysis showed that the vapor contained altogether only ∼6 mole percent of dimeric gold trichloride molecules and all the rest was chlorine gas. The presence of other species such as HCl, AuCl, Au_2Cl_2, and $AuCl_3$ was checked during the electron diffraction structure analysis and could be ruled out.

A 6 mol % presence of a sample in the vapor is usually not sufficient for a reliable structure determination by electron diffraction. However, the relative scattering power of the gold trichloride dimer is so much higher than that of the chlorine molecule that it allowed a rather reliable determination of the gold trichloride dimer molecular structure. Figure 1(a) shows the measured and calculated molecular intensities. The contribution of the 6% dimeric gold trichloride and that of the 94% chlorine, as calculated separately, are indicated in Figure 1(b). In the small scattering angle region, gold trichloride dominates. However, its intensity damps fast and at higher *s* values, the chlorine contribution becomes predominant. Figure 2 presents the radial distribution curves.

The electron diffraction experiments used 60 kV electrons and Kodak electron image plates. Five and six photoplates were selected for analysis at the 50 and 19 cm camera range, respectively. The data intervals at the 50 and 19 cm experiments are $s = 2-14$ Å^{-1} (with data steps of 0.125 Å^{-1}) and $s = 9-26.75$ Å^{-1} (with data steps of 0.25 Å^{-1}), respectively. Listings of the total electron diffraction intensities are available as Supporting Information. Tabulated electron scattering factors[17] were used in the analysis.

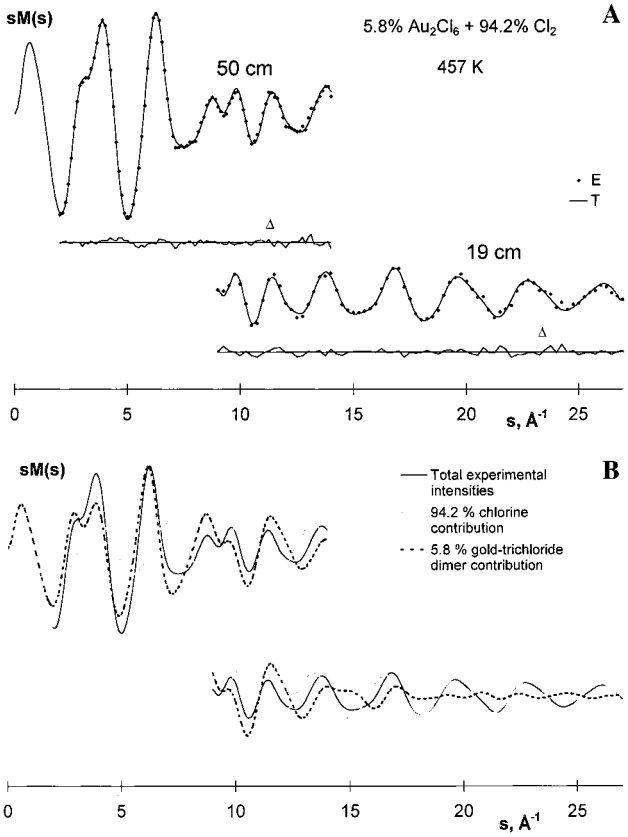

Figure 1. (a) Experimental (E) and calculated (T) molecular intensities of the Au_2Cl_6 and Cl_2 mixture at 457 K and their differences (Δ). (b) Contributions of Au_2Cl_6 and Cl_2 scattering to the total molecular intensities.

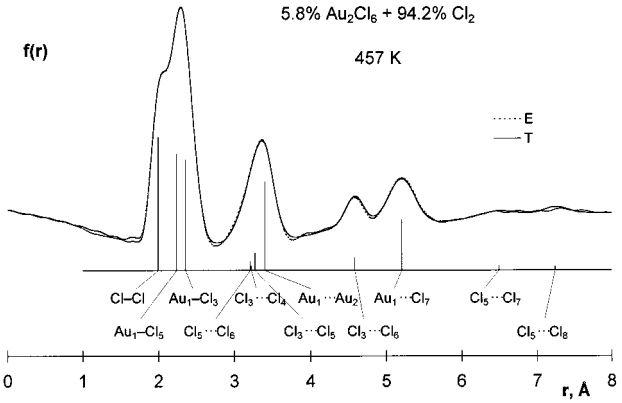

Figure 2. Experimental (E) and calculated (T) radial distributions of the Au_2Cl_6 and Cl_2 mixture at 457 K. The vertical bars indicate the relative contributions of different distances.

Due to the considerable decomposition already at low temperatures, it proved impossible to record the diffraction intensities for the monomer molecule at higher temperature. Therefore, to get a complete picture about the gas-phase structure of gold trichloride, high-level computations have been carried out on both the monomer and the dimer.

Computational Details

At first, computations were carried out on monomeric and dimeric gold trichloride. Different electronic states and geometries have been checked for the monomer because of the suggested Jahn−Teller effect. Multireference calculations at the CASSCF level were carried out, in which four electrons were correlated in six orbitals. Pseudopotential techniques were used for Au (for details, see below) and a standard 6-31G(d) basis

(11) Clinton, W. L.; Rice, B. *J. Chem. Phys.* **1959**, *30*, 542.
(12) Hargittai, M. *Chem. Rev.* **2000**, *100*, 2233.
(13) Hargittai, M.; Réffy, B.; Kolonits, M.; Marsden, C.; Heully, J.-L. *J. Am. Chem. Soc.* **1997**, *119*, 9042.
(14) Komiya, S.; Albright, T. A.; Hoffmann, R.; Kochi, J. K. *J. Am. Chem. Soc.* **1976**, *98*, 7255.
(15) Hargittai, I.; Tremmel, J.; Kolonits, M. *HSI Hung. Sci. Instrum.* **1980**, *50*, 31.
(16) Tremmel, J.; Hargittai, I. *J. Phys. E. Sci. Instrum.* **1985**, *18*, 148.
(17) Ross, A. W.; Fink, M.; Hilderbrandt, R.; Wang, J.; Smith, V. H., Jr. In *International Tables for Crystallography, C*; Wilson, A. J. C., Ed.; Kluwer: Dordrecht, 1995; pp 245−338.

set for chlorine. Four different planar states were investigated. The ground state is a singlet $^1A_1$ state, with C_{2v} symmetry, which indicates the presence of the Jahn−Teller effect. The next state is another C_{2v}-symmetry state (also of $^1A_1$ symmetry),which corresponds to the transition state with one imaginary frequency, and 6.1 kcal/mol higher in energy than the ground state. However, because the energy differences are rather sensitive to the applied basis sets and methods, higher level computations are more realistic in this respect (vide infra). The next state on the energy scale is a triplet D_{3h}-symmetry $^3E'$ state, and the highest energy one is a singlet D_{3h}-symmetry $^1E'$ state. The energy difference between the ground state and the open shell triplet is 28.6 kcal/mol; while the singlet D_{3h} state lies an additional 12.2 kcal/mol above the triplet state. The energy gap between the ground state and the triplet is much smaller than the one for the AuF_3 monomer (41.7 kcal/mol vs 28.6 kcal/mol here).

These calculations, as well as further higher level ones, were carried out with the Gaussian98 program package.[18] A multielectron adjusted quasirelativistic effective core potential covering 60 electrons ([Kr]4d^{10}4f^{14}) and an (8s7p6d)/[6s5p3d]-GTO valence basis set (311111,22111,411) of the Stuttgart group was used for gold.[19] Several all-electron basis sets were applied for chlorine, including 6-31G(d), 6-311+G(3d), 6-311+G(3df) and the Dunning correlation consistent cc-PVDZ and cc-PVTZ basis sets[20] augmented by diffuse functions. Full geometry optimizations were performed at two different correlated levels of theory, MP2 and density functional (B3LYP).[21] For the monomer ground-state, QCISD(T) and CCSD(T) calculations were also performed. All stationary points were characterized by a frequency analysis at both the B3LYP and the MP2 levels. Mulliken population analyses and NBO analyses[22] were carried out to investigate the bonding in both molecules at the MP2/6-31G(d) level.

The potential energy surface (PES) of $AuCl_3$ was calculated using the aug-cc-pVDZ basis set for chlorine. The energy was calculated as a function of the two Cl−Au−Cl angles in 5° steps. None of the determined points has been corrected for zero-point vibrations; such corrections are calculated to be rather small, of the order of 0.1−0.2 kcal/mol, in the harmonic approximation.

Calculations have also been carried out on AuCl and Au_2Cl_2 in order to help to check their possible presence in the vapor during the electron diffraction experiment. The structure of the $AuCl_4^-$ ion was calculated, in both the planar and a possible tetrahedral arrangement. We have also investigated the possibility of a nonplanar D_{2h}-symmetry dimer geometry (with two distorted tetrahedra sharing a common edge, as is typical for most metal trihalide dimers) to probe into the electronic origin of planarity of these systems.

Finally, we have calculated the energy potential (B3LYP and MP2 using a 6-31G(d) basis set for Cl) of the approach of two Jahn−Teller distorted monomers along a C_{2h} symmetry pathway forming either a planar or a nonplanar D_{2h}-symmetry dimer. To avoid basis set superposition error (BSSE),[23,24] the function counterpoise scheme of Boys and Bernardi[25] was used in this calculation, and the basis set of each monomer fragment was taken equal with the basis set of the dimer. During dimerization, both monomer fragments are distorted, and the calculated formation energy includes both the sum of the distortion energy of the fragments and BSSE. To separate those two factors, we used the scheme described by Timoshkin et al.[26]

The computed geometrical parameters for all of the molecules are collected in Table 1; the relative energies, in Table 2; and the computed frequencies for the ground-state species, in Table 3.

Electron Diffraction Analysis. The electron diffraction analysis was carried out applying certain constraints, on the basis of the quantum chemical calculations and experimental vibrational spectra.[27] In some refinements, the difference of the two different dimer bond lengths (bridging and terminal, see Figure 3) were taken over from the computation. Although the computed and experimental geometrical parameters have different physical meanings,[12,28,29] this is supposed to largely cancel in their differences and, thus, they can usually be carried over from computation to experiment with confidence. At the same time, according to our earlier experience,[30] it is important to check different levels of computations, because the changes of basis sets and methods of computation will have a varying impact on different geometrical parameters. According to Table 1, the difference in the dimer bond length scatters ∼0.03 Å, depending on the level of the computation. We have checked two values, 0.110 and 0.125 Å, from the highest level MP2 and B3LYP calculations, respectively. As to the actual bond lengths, the MP2/aug-cc-pVTZ-computed values are closer to the experimental ones than the B3LYP results.

A normal coordinate analysis was carried out[31] on the basis of the computed frequencies of the dimer. There is also experimental information on the molecular vibrations: four wavenumbers from a gas-phase infrared spectrum[27] and more from a crystal-phase study.[27] The computed MP2 frequencies agree much better with the experimental ones than the B3LYP values, in accordance with the shorter bond lengths in the former case. We also checked if scaling of these MP2 frequencies to

(18) Frisch, M. J.; Trucks, G. W.; Schlegel, H. B.; Scuseria, G. E.; Robb, M. A.; Cheeseman, J. R.; Zakrzewski, V. G.; Montgomery, J. A., Jr.; Stratmann, R. E.; Burant, J. C.; Dapprich, S.; Millam, J. M.; Daniels, A. D.; Kudin, K. N.; Strain, M. C.; Farkas, O.; Tomasi, J.; Barone, V.; Cossi, M.; Cammi, R.; Mennucci, B.; Pomelli, C.; Adamo, C.; Clifford, S.; Ochterski, J.; Petersson, G. A.; Ayala, P. Y.; Cui, Q.; Morokuma, K.; Malick, D. K.; Rabuck, A. D.; Raghavachari, K.; Foresman, J. B.; Cioslowski, J.; Ortiz, J. V.; Stefanov, B. B.; Liu, G.; Liashenko, A.; Piskorz, P.; Komaromi, I.; Gomperts, R.; Martin, R. L.; Fox, D. J.; Keith, T.; Al-Laham, M. A.; Peng, C. Y.; Nanayakkara, A.; Gonzalez, C.; Challacombe, M.; Gill, P. M. W.; Johnson, B.; Chen, W.; Wong, M. W.; Andres, J. L.; Gonzalez, C.; Head-Gordon, M.; Replogle, E. S.; Pople, J. A. Gaussian 98, Revision A.6; Gaussian, Inc.: Pittsburgh, PA, 1998.

(19) Andrae, D.; Häussermann, U.; Dolg, M.; Stoll, H.; Preuss, H. *Theor. Chim. Acta* **1990**, *77*, 123.

(20) (a) Woon, D. E.; Dunning, T. H. *J. Chem. Phys.* **1993**, *98*, 1358. (b) Kendall, R. A.; Dunning, T. H.; Harrison, R. J. *J. Chem. Phys.* **1992**, *96*, 6796. (c) Dunning, T. H. *J. Chem. Phys.* **1989**, *90*, 1007.

(21) (a) Becke, A. D. *J. Chem. Phys.* **1993**, *98*, 5648. (b) Lee, C.; Yang, W.; Parr, R. G. *Phys. Rev. B* **1988**, *37*, 785. (c) Miehlich, B.; Savin, A.; Stoll, H.; Preuss, H. *Chem. Phys. Lett.* **1989**, *157*, 200.

(22) (a) NBO Version 3.1, Glendening, E. D.; Reed, A. E.; Carpenter, J. E.; Weinhold, F. (b) Carpenter, J. E.; Weinhold, F. *J. Mol. Struct.* (*THEOCHEM*) **1988**, *169*, 41. (c) Foster, J. P.; Weinhold, F. *J. Am. Chem. Soc.* **1980**, *102*, 7211. (d) Reed, A. E.; Weinhold, F. *J. Chem. Phys.* **1983**, *78*, 4066. (e) Reed, A. E.; Weinstock, R. B.; Weinhold, F. *J. Chem. Phys.* **1985**, *83*, 735. (f) Reed, A. E.; Curtiss, L. A.; Weinhold, F. *Chem. Rev.* **1988**, *88*, 899. (g) Reed, A. E.; Schleyer, P. v. R. *J. Am. Chem. Soc.* **1987**, *109*, 7362. (h) Reed, A. E.; Schleyer, P. v. R. *Inorg. Chem.* **1988**, *27*, 3969. (i) Weinhold, F.; Carpenter, J. E. *The Structure of Small Molecules and Ions*; Plenum Press: New York, 1988; p 227.

(23) Clark, T. A. *Handbook of Computational Chemistry*; Wiley: New York, 1985.

(24) Klapötke, T. M.; Schulz, A. *Quantum Chemical Methods in Main-Group Chemistry*, with an invited chapter by R. D. Harcourt; John Wiley & Sons: Chichester, 1998.

(25) Boys, S. F.; Bernardi, F. *Mol. Phys.* **1970**, *19*, 553.

(26) Timoshkin, A. Y.; Suvorov, A. V.; Bettinger H. F.; Schaefer, H. F., III. *J. Am. Chem. Soc.* **1999**, *121*, 5687.

(27) Nalbandian, L.; Papatheodorou, G. N. *Vib. Spectrosc.* **1992**, *4*, 25.

(28) Bartell, L. S. *J. Chem. Phys.* **1955**, *23*, 1219.

(29) Hargittai, M.; Hargittai, I. *Int. J. Quantum Chem.* **1992**, *44*, 1057.

(30) Réffy, B.; Kolonits, M.; Hargittai, M. *J. Mol. Struct.* **1998**, *445*, 139.

(31) Hedberg, L.; Mills, I. M. *J. Mol. Spectrosc.* **1993**, *160*, 117.

Table 1. Computed Geometrical Parameters of Different Gold Chloride Species[a]

	level and basis for Cl[b]											
	B3LYP 6-31G(d)	B3LYP 6-311+ G(2d)	B3LYP 6-311+ G(3d)	B3LYP 6-311+ G(3df)	B3LYP aug-cc-PVDZ	B3LYP aug-cc-PVTZ	MP2 6-31G(d)	MP2 6-311+ G(3d)	MP2 aug-cc-PVDZ	MP2 aug-cc-PVTZ	QCISD(T) aug-cc-PVDZ	CCSD(T) aug-cc-PVDZ
$AuCl_3$, $^1A_1$, C_{2v} GS												
Au_1-Cl_2	2.292	2.282	2.284	2.268	2.289	2.265	2.277	2.268	2.274	2.213	2.288	2.288
Au_1-Cl_3	2.300	2.290	2.292	2.282	2.296	2.281	2.279	2.278	2.283	2.242	2.295	2.296
$\angle Cl_2-Au_1-Cl_3$	96.9	96.8	96.7	96.7	96.8	96.9	96.1	95.4	95.5	95.9	95.7	95.7
$AuCl_3$, $^1A_1$, C_{2v} TS												
Au_1-Cl_2	2.284	2.275	2.275	2.265	2.280	2.265	2.250	2.249	2.255	2.219		
Au_1-Cl_3	2.309	2.298	2.300	2.286	2.305	2.284	2.293	2.286	2.293	2.238		
$\angle Cl_2-Au_1-Cl_3$	137.6	137.9	138.1	138.1	138.1	138.1	138.0	138.9	139.1	138.6		
Au_2Cl_6, ^1A_g, D_{2h} GS[c]												
Au_1-Cl_5	2.303	2.297	2.298	2.287	2.302	2.287	2.288	2.284	2.288	2.244		
Au_1-Cl_3	2.442	2.424	2.423	2.415	2.428	2.412	2.410	2.395	2.397	2.354		
$\Delta(Au_1-Cl_3-Au_1-Cl_5)$	0.139	0.127	0.125	0.128	0.126	0.125	0.122	0.111	0.109	0.110		
$Au_1\cdots Au_2$	3.598	3.563	3.561	3.550	3.569	3.545	3.508	3.489	3.493	3.423		
$\angle Cl_3-Au_1-Cl_4$	85.1	85.4	85.4	85.4	85.4	85.2	86.6	86.5	86.5	86.7		
$\angle Cl_5-Au_1-Cl_6$	90.8	90.9	90.9	90.9	90.9	90.9	90.3	90.2	90.1	90.6		
Au_2Cl_6, ^1A_g, D_{2h} TS[d]												
Au_1-Cl_5	2.312		2.305		2.301	2.296	2.304	2.303	2.308			
Au_1-Cl_3	2.576		2.562		2.570	2.551	2.527	2.516	2.516			
$Au_1\cdots Au_2$	3.441		3.395		3.423	3.397	3.077	3.046	3.053			
$\angle Cl_3-Au_1-Cl_4$	96.2		97.0		96.5	96.5	105.0	105.5	105.3			
$\angle Cl_5-Au_1-Cl_6$	165.7		166.4		165.9	165.9	165.6	168.3	167.5			
$AuCl_4^-$, $^1A_{1g}$, D_{4h} GS												
$Au-Cl$	2.364	2.357	2.357	2.347	2.361	2.346	2.336	2.333	2.337	2.293		
$AuCl_4^-$, $^3B_{2g}$, D_{4h}												
$Au-Cl$	2.482		2.471		2.478	2.462	2.432	2.424	2.429	2.354		
$AuCl_4^-$, $^1T_2$, T_d												
$Au-Cl$	2.453		2.445		2.453	2.430	2.428	2.428	2.431	2.364		
$AuCl_4^-$, $^3T_2$, T_d												
$Au-Cl$	2.453		2.446		2.453	2.432	2.409	2.406	2.412	2.354		
$AuCl_4^-$, $^1A_1$, D_{2d}												
$Au-Cl$	2.444		2.436		2.442	2.421	2.411	2.407	2.411	2.351		
$\angle Cl-Au-Cl$	92.1		91.7		91.7	91.6	92.0	89.8	89.6	89.8		
$AuCl_4^-$, $^3A_1$, D_{2d}												
$Au-Cl$	2.445		2.438		2.444	2.424	2.401	2.397	2.400	2.348		
$\angle Cl-Au-Cl$	89.7		89.4		89.3	89.5	90.6	88.7	88.5	88.9		
$AuCl_4^-$, $^1A_1$, C_{2v}												
$Au-Cl_1$	2.516		2.513		2.520	2.503	2.461	2.465	2.467	2.422		
$Au-Cl_3$	2.372		2.360		2.366	2.340	2.348	2.339	2.344	2.274		
$\angle Cl_1-Au-Cl_2$	98.0		97.5		97.6	97.0	101.1	98.7	99.0	97.8		
$\angle Cl_3-Au-Cl_4$	87.7		87.2		87.1	87.1	85.4	83.2	82.9	83.3		
AuCl, $^1\Sigma_g$												
$Au-Cl$	2.286	2.281	2.282	2.266	2.289	2.263	2.269	2.273	2.282	2.218		
Au_2Cl_2, ^1A_g												
$Au-Cl$	2.567	2.552	2.552	2.543	2.559	2.537	2.540	2.529	2.531	2.469		
$Au\cdots Au$	2.823	2.815	2.813	2.809	2.818	2.804	2.786	2.800	2.803	2.769		
$\angle Cl-Au-Cl$	113.3	113.1	113.1	112.9	113.2	112.9	113.5	112.8	112.7	111.8		

[a] Distances in angstroms, angles in degrees. For numbering of atoms, see Figure 3. GS, ground-state geometry; TS, transition-state geometry. [b] Basis for Au: a multielectron-adjusted quasirelativistic effective core potential covering 60 electrons ([Kr]$4d^{10}4f^{14}$) and an (8s7p6d)/[6s5p3d]-GTO valence basis set (311111,22111,411).[19] [c] Planar geometry; see Figure 3. [d] Distorted tetrahedral geometry; see Figure 3.

the available few gas-phase values makes any difference, but the vibrational amplitudes were insensitive to this amount of change in the frequencies. The initial values of all of the vibrational amplitudes were taken from the normal coordinate analysis; those of the bond lengths and nonbonded distances with large multiplicity were later varied, the others were kept unchanged. Both the MP2 and the B3LYP amplitudes were checked. The refinement of the vibrational amplitudes resulted in a better agreement with the MP2 values than with the B3LYP results. Since the MP2 bond length difference proved also to be better (vide infra), eventually the MP2 based vibrational amplitudes were accepted for those distances whose amplitudes could not be refined.

The structure refinement was carried out assuming a lower, C_{2v}, symmetry for the dimer to allow for the shrinkage effect[32] in the same way that it was done for Au_2F_6.[2] The apparent puckering angle of the four-membered ring was very sensitive to the refinement scheme and could only be refined if the relative abundance of the molecular species was kept constant. Its final value was achieved with subsequent refinement steps; most parameters, except the bond angles, were insensitive to the value of this angle. Due to the small relative abundance of gold trichloride in the vapor, a so-called dynamic analysis was not attempted, but dynamic intramolecular multiple scattering was included in the analysis. These corrections were calculated by the MUSCAT[33] program based on Glauber's theory[34] and modified by Bartell's intratarget propagation model.[35] The

(32) See, for example, Kuchitsu, K. In *Diffraction Studies on Non-Crystalline Substances*; Hargittai, I., Orville-Thomas, W. J., Eds.; Elsevier: Amsterdam, 1981; pp 63−116.

Table 2. Energies

	level and basis for Cl							
	B3LYP 6-31G(d)	B3LYP 6-311+G(3d)	B3LYP aug-cc-PVDZ	B3LYP aug-cc-PVTZ	MP2 6-31G(d)	MP2 6-311+G(3d)	MP2 aug-cc-PVDZ	MP2 aug-cc-PVTZ
Relative Energies, Distortion Energies, Dimerization Energies, and BSSE for Different Gold Chloride Molecules (kcal/mol)[a]								
Δ_0E ($AuCl_3$, TS−GS)	2.9	2.6	2.5	2.3	2.9	2.1	1.8	1.8
$\Delta_{298}H$ ($AuCl_3$, TS−GS)	2.3	2.0	1.9	1.7	2.3	1.5	1.2	1.2
Δ_0E (Au_2Cl_6, TS−GS)	58.5	61.3	61.1	64.1	65.6	67.4	68.4	
$\Delta_{298}H$ (Au_2Cl_6, TS−GS)	57.8	60.4	60.3	63.3	64.7	66.5	67.4	
E^{dist} ($AuCl_3$, GS)[b]	3.9	3.6	3.6	3.8	3.7	2.9	2.9	3.2
E^{dist} ($AuCl_3$, TS)[c]	9.1	9.1	9.2	10.0	8.5	9.1	9.2	
E^{BSSE} ($AuCl_3$, GS)	1.5	1.6	1.1	0.5	8.1	6.9	6.2	6.0
Δ_0E ($AuCl_3$, dimeriz.)	−47.1	−50.1	−48.8	−48.4	−61.6	−68.1	−67.3	−70.8
$\Delta_{298}H$ ($AuCl_3$, dimeriz.)	−45.8	−48.7	−47.5	−47.0	−60.2	−66.8	−65.9	−69.4
$\Delta_{298}H^{BSSE\ corr}$ ($AuCl_3$, dimeriz.)	−42.9	−45.5	−45.4	−46.0	−44.0	−53.0	−53.5	−57.3
E^{dist} (AuCl)	7.8	6.9	6.7	7.3	7.3	6.9	6.8	7.6
E^{BSSE} (AuCl)	0.6	0.5	0.3	0.2	6.2	5.1	4.9	4.8
Δ_0E (AuCl, dimeriz.)	−24.1	−21.4	−21.3	−19.4	−29.1	−32.1	−31.8	−31.5
$\Delta_{298}H$ (AuCl, dimeiz.)	−23.6	−20.9	−20.8	−18.9	−28.6	−31.6	−31.3	−31.0
$\Delta_{298}H^{BSSE\ corr}$ (AuCl, dimeriz.)	−22.4	−19.9	−20.3	−18.6	−16.2	−21.4	−21.5	−21.4
Relative Energies of Different $AuCl_4^-$ Species (kcal/mol)								
$AuCl_4^-$, $^1A_{1g}$, D_{4h} GS	0.0	0.0	0.0	0.0	0.0	0.0	0.0	0.0
$AuCl_4^-$, $^3B_{2g}$, D_{4h}	37.8	38.6	38.2	42.1	60.6	60.7	60.9	63.9
					58.6[d]	58.4[d]	60.9[d]	61.8[d]
$AuCl_4^-$, $^1T_2$, T_d	54.1	55.6	55.0	57.3	61.5	65.8	65.3	69.3
$AuCl_4^-$, $^3T_2$, T_d	42.1	43.6	43.0	45.3	55.4	59.9	59.2	62.5
					52.9[d]	57.3[d]	56.6[d]	60.2[d]*
$AuCl_4^-$, $^1A_1$, D_{2d}	51.1	52.3	51.7	53.9	59.1	61.9	61.4	64.5
$AuCl_4^-$, $^3A_1$, D_{2d}	35.2	36.5	35.9	37.9	47.2	50.4	49.8	52.5
					44.6[d]	47.8[d]	47.2[d]	50.2[d]
$AuCl_4^-$, $^1A_1$, C_{2v}	48.2	49.2	48.7	50.5	55.9	58.4	57.9	60.0

[a] GS: ground state; TS: transition state. [b] $AuCl_3$ monomer unit in Au_2Cl_6 GS. [c] $AuCl_3$ monomeric unit in Au_2Cl_6 TS. [d] Spin projected values, PMP2.

contribution of multiple scattering to the total experimental intensity appeared to be less important than it was for the Au_2F_6 dimer. Due to the small contribution of the Au_2Cl_6 scattering to the total intensity at higher s-values, the possible anharmonicity associated with the gold−chlorine bond lengths could not have any appreciable effect and, thus, was neglected.

The chlorine molecule is the major component of the gas phase. Because the structure of this molecule is well-known,[36] the vibrational amplitude and asymmetry parameter of chlorine (l_{Cl-Cl} = 0.049 Å, $\kappa_{Cl-Cl} = 1.6 \times 10^{-6}$ Å^3) were calculated from spectroscopic constants.[36b] These parameters were kept unchanged in order to decrease unnecessary correlations among the parameters. The bond length of Cl−Cl was refined, keeping the difference of the Au−Cl bond length difference unchanged. Using the MP2 value for this difference, 0.110 Å, gave better agreement for the chlorine bond length, r_g 1.992 ± 0.004 Å, with previously published values than it did with the B3LYP value. Previous values are the r_g from electron diffraction (1.993 ± 0.003 Å)[36a] and the r_e from rotational spectroscopy (1.988 Å),[36b] with the latter converted to r_g (1.994 Å) with appropriate corrections.

In the last stage of the analysis, the chlorine bond length was assumed at the literature value, as were the vibrational amplitudes of the two Au−Cl distances at the calculated values, to refine the bond length difference of the two Au−Cl distances. The result was 0.118 ± 0.024 Å. The geometrical parameters are given in Table 4.

Discussion

Gold Trichloride Monomer. The monomeric $AuCl_3$ molecule has a Jahn−Teller distorted structure similar to AuF_3 (see Figure 3). The highest symmetry D_{3h} nuclear configuration of such a molecule, with gold in a d^8 electronic configuration and in an E' electronic state, can be considered as an ($E \times e$) Jahn−Teller case, which is similar to the much-studied ($E \times e$) problem in octahedral systems.[37] In the octahedral case, the distortion results in a D_{4h} structure, while the D_{3h} trigonal planar molecule distorts to a C_{2v} geometry. Distortion of the lower lying triplet $^3E'$ state would not bring about any energy gain, but the singlet $^1E'$ is subject to Jahn−Teller distortion. Although the energy difference between these two states is ∼12 kcal/mol (CASSCF level), the Jahn−Teller stabilization energy for the singlet is as much as 41 kcal/mol and, thus, it can more than compensate for the spin pairing. Figure 4 shows the relative energies for these states. Apparently, relativistic effects enhance the driving force toward this distortion by lowering the energy of the 6s orbitals and making the 5d orbitals the major contributor to the valence shell. The enhanced role of 5d orbitals explains the greater angular distortion in AuF_3 and $AuCl_3$, as compared to that in MnF_3 (see Table 5).

If only linear terms were important in the vibronic interaction for this $E-e$ problem, the adiabatic potential would show a typical Mexican-hat surface with an equal-depth "brim" of the hat around the central maximum. However, if the quadratic terms are also important in this vibronic interaction, the surface of the brim warps, producing three wells separated by three humps of equal height. It is this latter type that $AuCl_3$ (similarly to AuF_3) exhibits, showing the importance of the quadratic terms in the vibronic interaction. There are three equivalent minima

(33) Intramolecular Multiple Scattering Program by Miller, B. R. (see ref 35).

(34) Glauber, R. J. In *Lectures in Theoretical Physics, Vol. I*; Brittin, W. E., et al., Eds; Interscience: New York, 1959.

(35) Miller, B. R.; Bartell, L. S. *J. Chem. Phys.* **1980**, *72*, 800.

(36) (a) Shibata, S. *J. Phys. Chem.* **1963**, *67*, 2256. (b) Huber, K. P.; Herzberg, G. *Molecular Spectra and Molecular Structure*: *IV. Constants of Diatomic Molecules*; Van Nostrand Reinhold: New York, 1979.

(37) See, for example, Bersuker, I. B. *Electronic Structure and Properties of Transition Metal Compounds*; John Wiley & Sons: New York, 1996.

Table 3. Vibrational Frequencies (cm^{-1}), Symmetry Assignments, and Infrared Intensities (km/mol) of the Ground-State Structures of Au_2Cl_6, $AuCl_3$, $AuCl_4^-$, AuCl, and Au_2Cl_2

		MP2 6-31(d)	B3LYP 6-31(d)	B3LYP aug-cc-PVTZ	experiment gas[a]	experiment solid[a]
Au_2Cl_6	A_g	373(0)	360(0)	366(0)	386	378
		314(0)	295(0)	305(0)	324	327
		161(0)	151(0)	150(0)	157	166
		93(0)	87(0)	87(0)	96	97
	A_u	55(0)	57(0)	60(0)		
	B_{1g}	372(0)	353(0)	359(0)		365
		279(0)	245(0)	260(0)		288
		121(0)	113(0)	115(0)		122
	B_{1u}	130(1)	132(1)	138(1)		135
		16(1)	32(1)	34(1)		44
	B_{2g}	100(0)	101(0)	105(0)		104
	B_{2u}	380(11)	363(20)	369(22)		383
		293(4)	268(2)	282(2)		313
		86(0.3)	82(0)	82(0)		80
	B_{3g}	95(0)	98(0)	103(0)		
	B_{3u}	369(57)	355(64)	361(66)		373
		302(84)	268(58)	283(54)		309
		156(2)	147(1)	144(1)		143
$AuCl_3$	A_1	363(0)	343(1)			
		353(0)	334(0)			
		118(1)	115(1)			
	B_1	111(3)	104(2)			
	B_2	396(65)	370(53)			
		80(0)	68(0)			
$AuCl_4^-$	A_{1g}	327(0)	305(0)			
	A_{2u}	129(5)	126(5)			
	B_{1g}	311(0)	281(0)			
	B_{2g}	160(0)	152(0)			
	B_{2u}	75(0)	71(0)			
	E_u	356(64)	326(65)			
		153(0)	149(0)			
AuCl	Σ_g	353(20)	328(10)			
Au_2Cl_2	A_g	281(0)	257(0)			
		92(0)	81(0)			
	B_{3g}	90(0)	79(0)			
	B_{1u}	99(49)	108(31)			
	B_{2u}	241(55)	216(43)			
	B_{3u}	66(6)	67(4)			

[a] From ref 27.

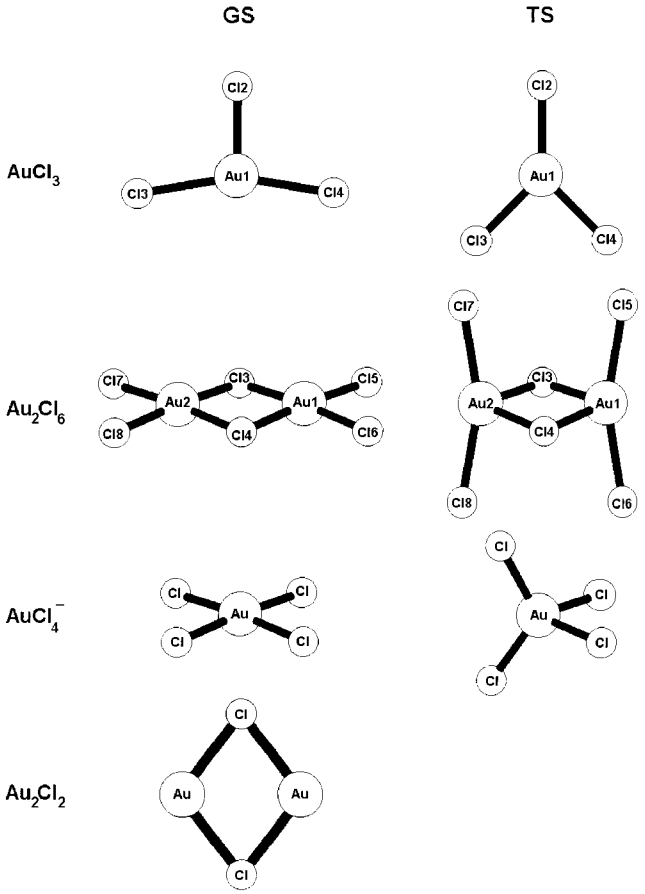

Figure 3. Molecular models and numbering of atoms in $AuCl_3$ (ground state and transition state), Au_2Cl_6 in planar and distorted tetrahedral coordination, $AuCl_4^-$ in planar and tetrahedral coordination, and Au_2Cl_2 dimer. Left side, ground-state molecules; right side, saddle point ($AuCl_3$ and Au_2Cl_6) and other higher energy geometries ($AuCl_4^-$).

[E_{min1}(96.8°,166.4°), E_{min2}(166.4°, 96.8°), and E_{min3}(96.8°, 96.8°)] and three saddle points, the latter corresponding to the transition states. The D_{3h} global maximum is in the center of the two-dimensional potential energy surface and corresponds to the undistorted $AuCl_3$ molecule (see Figure 5). The transition states describe the change of an equatorial chlorine atom into an axial atom. The PES of $AuCl_3$ is more shallow, and the energy barrier between the ground-state and the transition-state structures is smaller than in AuF_3 (at the B3LYP/aug-cc-PVDZ level: AuF_3, $\Delta E = 5.4$; $AuCl_3$, $\Delta E = 2.3$ kcal/mol).

It is instructive to compare the Jahn−Teller distortion in gold trichloride and gold trifluoride, both in their ground state and transition state. Table 5 shows the geometries, from B3LYP and MP2 level computations.

The type of distortion in the ground state is the same for both molecules, which results in a T-shaped structure with one short and two longer bonds and two smaller and one larger angle (see Figure 3). The only difference is that the distortion is slightly larger in AuF_3, both in the bond angles and the bond lengths, than it is in $AuCl_3$.

NPA population analysis indicates that it is the Au 5d orbitals that are the major contributors to the bonding, and there is only a small 6s participation and practically no 6p contribution (see Table 6). An interesting feature is the apparently fairly large amount of π bonding. As Figure 6 indicates, there are both in-plane and out-of-plane π orbitals, with back-bonding in both molecules, but the overlap is larger in the trifluoride than in the trichloride. Although the fact that the Au_1-X_2 bond is shorter than the other two is rationalized by the Jahn−Teller active vibration, which brings about the C_{2v}-symmetry ground-state structure, the population of these π MOs enhances this effect. The Au_1-X_2 bond is a two-center π bond (HOMO-9 and HOMO-10 for AuF_3 and $AuCl_3$, respectively), whereas the Au_1-X_3 and Au_1-X_4 bonds are three-center bonds (HOMO-11). The b_2 symmetry MO (HOMO-12) describes a four-center in-plane π bond.

The transition state geometries are somewhat different in the trifluoride and trichloride molecules. Although in both cases the bond angles correspond to the expected Jahn−Teller distortion of the opposite phase (i.e., two large and one small bond angle) as compared to the ground-state structures, in $AuCl_3$ the relationship of the bond lengths remains the same as in the case of the ground-state structure (i.e., one short and two long bonds). A possible reason is the larger size of the chlorine atoms, as compared with fluorine, and the very short Cl···Cl nonbonded distance in the molecule. The Cl···Cl distance is 2.960 and 3.051 Å (MP2 and B3LYP values, both with aug-cc-pVTZ basis on Cl, respectively) in the transition-state molecule. This is considerably shorter then the same 1,3 nonbonded Cl···Cl distances in other molecules. Excluding first-row central atoms, the 1,3 Cl···Cl distances range between 3.12 and 3.79 Å and are longer than 3.5 Å if we consider only molecules with larger metal atoms, such as Bi or Pb. Thus, the Cl···Cl distance in gold trichloride is extremely short, even with the longer than expected bond lengths of this transition-state molecule. Another

Table 4. Geometrical Parameters[a] of Au_2Cl_6[b] and Cl_2 from Electron Diffraction

parameter	ED		NCA[c]
	r_g	l	l
Au_1-Cl_5	2.236 ± 0.013	0.054[d]	0.054
Au_1-Cl_3	2.355 ± 0.013	0.070[d]	0.070
$\Delta[(Au_1-Cl_3)-(Au_1-Cl_5)]$	0.118 ± 0.024		
$Au_1\cdots Au_2$	3.404 ± 0.013	0.096 ± 0.044	0.092
$Au_1\cdots Cl_7$	5.207 ± 0.013	0.124 ± 0.051	0.126
$Cl_3\cdots Cl_5$	3.277 ± 0.083	0.151 ± 0.062	0.145
$Cl_3\cdots Cl_6$	4.588 ± 0.010	0.077 ± 0.040	0.085
$\angle_a Cl_5-Au_1-Cl_6$	91.7 ± 2.5		
$\angle_\alpha Cl_5-Au_1-Cl_6$	92.7 ± 2.5		
$\angle_a Cl_3-Au_1-Cl_4$	86.5 ± 1.8		
$\angle_\alpha Cl_3-Au_1-Cl_4$	86.8 ± 1.8		
$\angle_a$[e]	14.0		
dimer %	5.8 ± 0.3		
Cl−Cl[f]	1.994	0.049	0.049

[a] Bond lengths and vibrational amplitudes in Å, angles in degrees. Error limits are estimated total errors, including systematic errors, and the effect of constraints used in the refinement, $\sigma_t = (2\sigma_{LS}^2 + (cp)^2 + \Delta^2)^{1/2}$, where σ_{LS} is the standard deviation of the least-squares refinement, p is the parameter, c is 0.002 for distances and 0.02 for amplitudes, and Δ is the effect of constraints. For numbering of atoms, see Figure 3. [b] Assumed model symmetry C_{2v}, allowing for shrinkages (the equilibrium structure has D_{2h} symmetry). [c] Vibrational amplitudes calculated by normal coordinate analysis. [d] Value taken from normal coordinate analysis. [e] Apparent puckering angle of the four-membered ring of the dimer. Parameter refined with a trial-and-error method. [f] Parameters of Cl_2 taken from ref 36b and converted to our experimental conditions. Refinement with constrained Δ(Au−Cl) resulted in r_g(Cl−Cl) = 1.992 ± 0.004 Å.

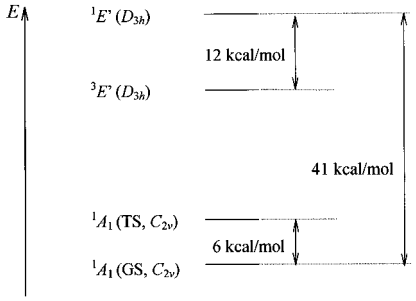

Figure 4. Energy differences (arbitrary scale) between different electronic states of $AuCl_3$ computed at the CASSCF(4,6) level. For applied basis sets, see Computational Details.

Table 5. Geometrical Parameters Indicating the Jahn−Teller Distortion in MnF_3, AuF_3, and $AuCl_3$, Based on B3LYP and MP2 Computations[a]

	MnF_3[b]		AuF_3[c]		$AuCl_3$[d]	
	B3LYP	MP2	B3LYP	MP2	B3LYP	MP2
ground state						
M_1-X_2	1.734	1.726	1.890	1.846	2.265	2.213
M_1-X_3	1.755	1.752	1.910	1.881	2.281	2.242
$\angle X_2-M_1-X_3$	106.6	105.7	94.3	92.8	96.9	95.9
transition state						
M_1-X_2	1.770	1.773	1.915	1.880	2.265	2.219
M_1-X_3	1.741	1.731	1.895	1.861	2.284	2.238
$\angle X_2-M_1-X_3$	128.4	129.1	139.3	140.2	138.1	138.6

[a] The reference (undistorted) symmetry is D_{3h}. [b] All electron TZ bases were applied for both atoms. For detailed information, see ref 13. [c] aug-cc-PVTZ basis was used for fluorine and an unpublished Stuttgart quasirelativistic ECP and valence basis augmented with additional *d* and *f* polarization functions for gold. See ref 2. [d] aug-cc-PVTZ basis was used for chlorine and a Stuttgart-type quasirelativistic ECP and valence basis for gold. This work.

interesting feature of this structure is the actual overlap between the 3s orbitals of the two chlorine atoms, as shown in Figure 7, which may be either a consequence or a reason for this short 1,3 distance.

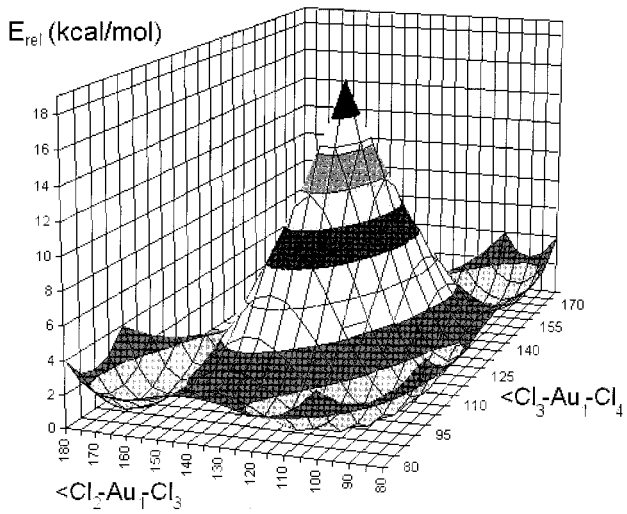

Figure 5. Mexican-hat-type potential energy surface of $AuCl_3$. Computation at the B3LYP level. Cl basis set, aug-cc-pVDZ.

Gold Trichloride Dimer. According to the present work, the dimer of gold trichloride has a planar D_{2h}-symmetry halogen-bridged structure, which is in contrast to most metal halide dimers in which the metals have a distorted tetrahedral configuration.[12] This planarity has been observed for Au_2F_6 in the gas phase[2] and for Au_2Cl_6 in its crystal.[3,4] Lower level computations had also suggested such a structure.[3] The Jahn−Teller effect cannot be the reason for the planar geometry, because the two types of structures have the same symmetry (in addition the tetrahedral structure's having a nondegenerate state). To understand the origin of the planar geometry, we investigated both the planar and the usual nonplanar geometry, the latter consisting of two distorted tetrahedra sharing an edge, both molecules with D_{2h} symmetry (see Figure 3). The nonplanar structure does not represent a minimum on the PES of Au_2Cl_6; rather, it is a transition state, with one imaginary frequency, that describes the exchange of one chlorine atom between the two monomeric units. The structural parameters of this nonplanar saddle-point geometry indicate that the distortion of the T-shaped $AuCl_3$ monomers is relatively small, resulting in an unusually large $Cl_5-Au_1-Cl_6$ angle of 166°, which is in contrast to the usual angle of ∼120° in such molecules.[12] Energetically, the nonplanar dimer lies ∼64 kcal/mol (B3LYP/aug-cc-pVTZ, see Table 2) above the planar configuration. The almost T-shaped structure of the monomer is well-preserved in the planar dimer as well, considering that the $Cl_3-Au_1-Cl_6$ angle is ∼177°. The estimated distortion energies (B3LYP/aug-cc-pVTZ) of 3.8 kcal/mol per monomer unit for the planar dimer and 10.0 kcal/mol per monomer unit for the distorted tetrahedral dimer favor the formation of the planar species (see Table 2). Our calculations of the approach of two $AuCl_3$ monomers show that no bonding occurs in the nonplanar case (energy potential leads to a maximum), whereas the planar molecule (potential leads to a minimum) is formed without an activation barrier.

There are alternative explanations for the planarity of Au_2Cl_6 in the literature. A typical textbook argument is that dsp^2 hybridization rather than sp^3 takes place in the molecules of d^8 metals, and that favors planar coordination.[38] An earlier computation, based on Mulliken population analysis, supported this idea.[3] Our results, however, are at variance with such an interpretation, at least for the gold halides. Table 6 shows the

(38) Wells, A. F. *Structural Inorganic Chemistry*, 4th ed.; Clarendon Press: Oxford, 1975; p 909.

Table 6. Natural Population Analysis (NPA, NBO program) and Gross Atomic Populations (GAP, Mulliken Population Analysis) and Natural Electron Configuration and NBO Charges of the Gold Atom in Different Gold Chlorides (Ground States)[a]

	6s	$6p_x$	$6p_y$	$6p_z$	$5d_{xy}$	$5d_{xz}$	$5d_{yz}$	$5d_{x^2-y^2}$	$5d_{z^2}$	nat. electron config.
AuCl										
NPA	0.39509	0.00831	0.00831	0.00738	1.99993	1.99707	1.99707	1.99993	1.90587	[core]6s(0.40)5d(9.90)6p(0.02)
GAP	0.49560	0.04542	0.04542	0.05146	1.99990	2.01026	2.01026	1.99990	1.91179	q(Au) = +0.679
Au_2Cl_2										
NPA	0.26926	0.00022	0.00027	0.00582	1.99945	1.99965	1.99380	1.95449	1.99584	[core]6s(0.27)5d(9.94)6p(0.01)
GAP	0.41485	0.03346	0.16835	0.00557	2.01483	2.00039	1.99204	1.96108	1.97779	q(Au) = +0.760
$AuCl_4^-$										
NPA	0.57123	0.00108	0.00108	0.00278	1.99808	1.99861	1.99861	1.22108	1.96402	[core]6s(0.57)5d(9.18)6p(0.01)
GAP	0.65567	0.18586	0.18586	0.09571	2.06519	2.03658	2.03658	1.2615	1.97557	q(Au) = +1.182
$AuCl_3$										
NPA	0.54295	0.00927	0.01983	0.01544	1.99867	1.99902	1.99789	1.73665	1.49516	[core]6s(0.54)5d(9.23)6p(0.04)
GAP	0.63238	0.07949	0.15046	0.12878	2.03567	2.00702	2.05562	1.75999	1.51037	q(Au) = +1.174
Au_2Cl_6										
NPA	0.57916	0.00897	0.00011	0.01871	1.99828	1.99806	1.25742	1.97220	1.98951	[core]6s(0.58)5d(9.22)6p(0.03)
GAP	0.67281	0.08941	0.14664	0.19968	2.02145	2.01409	1.27937	1.99157	1.97150	q(Au) = +1.144

[a] MP2 method with a 6-31G(d) basis set for chlorine.

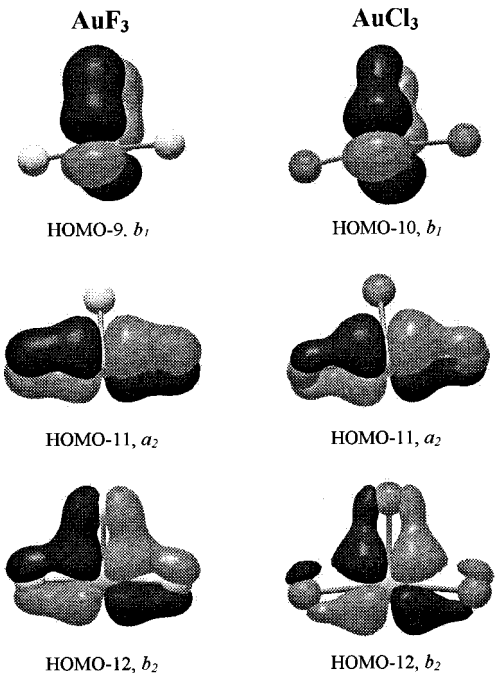

Figure 6. Comparison of some bonding molecular orbitals of the ground-state monomers of AuF_3 and $AuCl_3$ (MP2/6-31G(d) for Cl).

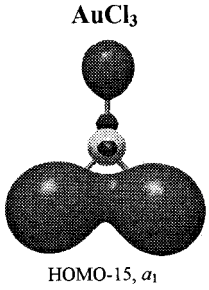

Figure 7. Orbital overlap of chlorine s orbitals in the transition-state structure of $AuCl_3$ (MP2/6-31G(d) for Cl).

results of population analyses by the NPA[22] method and the Mulliken method. The major difference between the two is in the role of 6p orbitals; although the Mulliken analysis gives a noticeable 6p contribution, the NPA does not. There have been prior warnings about the reliability of the Mulliken analysis, especially in molecules with transition metals.[22e] It seems that the NPA results are more reliable and show practically no contribution from the 6p orbitals to the bonding; thus, the idea

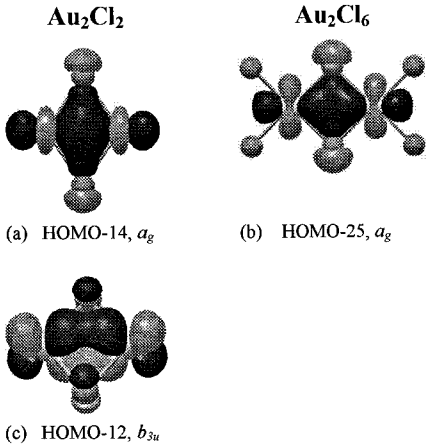

Figure 8. Molecular orbitals showing intra-ring Au···Au interactions in Au_2Cl_2 and Au_2Cl_6.[39] Closed four-center bonds in (a) Au_2Cl_2 and (b) Au_2Cl_6 (this is the lowest lying σ MO of Au_2Cl_6) (c) dπ−dπ interaction in Au_2Cl_2 (MP2/6-31G(d) for Cl).

of dsp^2 hybridization as the reason for the planar geometry in Au_2Cl_6 does not hold.

One of the origins of this planarity is relativistic effects. They bring about the contraction of the 6s and the expansion of the 5d orbitals. Due to this effect, the 5d orbitals, rather than being simply nonbonding, will be the major contributors to the valence shell, with only a small amount of 6s present (see Table 6). The shape of these orbitals favors the planar arrangement over the tetrahedral one. There are other interesting features in this dimer. Thus, there is a definite Au···Au interaction, which is considerably superimposed with the Au−Cl bridging bonds. This interaction can be regarded as a closed 4-center bond with the largest coefficients on the Au atoms (HOMO-25, a_g, see Figure 8b). This MO of a_g symmetry represents a linear combination involving mainly $5d_{z^2}$ and $5d_{x^2-y^2}$ orbitals of the Au atoms and 3p orbitals of the Cl atoms.[39b] It is interesting to note that this bonding molecular orbital represents the lowest lying σ bond that can be considered as a synergistic AuAu and AuCl σ-type interaction.

In summary, the different factors leading to the planar arrangement in the dimer are (i) The distortion of the Jahn−

(39) (a) $\Psi^{HOMO-14} \approx -0.25\ 3p_y(Cl_3) + 0.25\ 3p_y(Cl_4) + 0.66\ 5d_{z2}(Au_1) + 0.66\ 5d_{z2}(Au_2)$; (b) $\Psi^{HOMO-25} \approx -0.24\ 3p_y(Cl_3) + 0.24\ 3p_y(Cl_4) + 0.63\ 5d_{z2}(Au_1) + 0.63\ 5d_{z2}(Au_2) + 0.20\ 5d_{x2-y2}(Au_1) + 0.20\ 5d_{x2-y2}(Au_2)$; (c) $\Psi^{HOMO-12} \approx 0.67\ 5d_{xz}(Au_1) - 0.67\ 5d_{xz}(Au_2) - 0.25\ 3p_x(Cl_3) - 0.25\ 3p_x(Cl_4)$. Only coefficients >0.1 are considered; both molecules lie in the *yz* plane with bridging Cl atoms on the *y* axis and Au_1 and Au_2 on the *z* axis.

Teller-affected monomer to form a tetrahedral dimer costs a larger amount of energy than to form the planar one. The tetrahedral dimer has a strange shape with a very large angle between the terminal chlorine atoms, ~166°, and is not a minimum structure. (ii) There are favorable orbital overlaps in the planar dimer, such as the Au···Au interaction, a certain amount of π bonding, and several nonbonding interactions among the chlorine atoms. (iii) There is unfavorable electrostatic repulsion between bonding and nonbonding electron pairs in the nonplanar species. A recent paper, based on simple ion model calculations, attributes the planarity of Au_2Cl_6 to the quadrupolar polarizability of gold(III).[40]

When the experimental electron diffraction and the computed geometries for the dimer are compared, the MP2 level triple-ζ basis results give the best agreement with the bond lengths. The experimental bond angles agree with all of the computed values within the experimental uncertainties. Generally speaking, the MP2 level reproduces the experimental bond lengths better than the B3LYP, and the inclusion of *f* polarization functions shortens the computed bond lengths considerably, bringing them closer to the experimental values. Comparison of our gas-phase geometry to the crystal structure[3,4] shows a general agreement, again, within experimental errors.

$AuCl_4^-$. The planarity of the Au_2X_6 (X = F, Cl) dimers is in line with the planarity of the MX_4^- ions of Au(III) and other d^8 transition metals, such as Ni(II), Pd(II), and Pt(II). The $AuCl_4^-$ ions appear frequently in crystals, and they are invariably planar. The average Au−Cl bond length is 2.27 Å in 24 observed structures containing the $AuCl_4^-$ ion.[9b] Our computed values, depending on the level of computation, vary between 2.29 and 2.36 Å; that is, they are longer yet than the experimental ones. Again, the MP2 method with the aug-cc-pVTZ basis for chlorine seems to give the best agreement. It should be noted that the computation was carried out for the single, isolated (gas-phase) ion. Therefore, certain differences from the X-ray diffraction results can be expected.

The tetrahedral structure of the $AuCl_4^-$ ion, with its T_2 electronic state, is subject to the Jahn−Teller effect. Nonetheless, the appearance of a square-planar arrangement cannot be explained with this effect, since the D_{4h} point group is not a subgroup of T_d; thus, the molecule cannot distort to that symmetry.[41] The shape and occupation of molecular orbitals provide a straightforward explanation of the planar coordination in this ion. There are favorable orbital overlaps at both the σ and π levels in this arrangement, as shown in Figure 9. On the other hand, in the tetrahedral configuration the d orbitals localized on the Au center are not directed along the Au−Cl bonds, and thus, they do not provide such a favorable overlap as for the planar arrangement.

The energy difference between the ground-state D_{4h} singlet molecule and the tetrahedral arrangement is rather high, between 54 and 69 kcal/mol, depending on the method of calculation. Because the T_d structure, both the singlet and the triplet, is subject to Jahn−Teller distortions, it is interesting to see which geometries they distort to. The 3-fold degenerate T_2 state of this molecule gives a complicated Jahn−Teller surface of many dimensions. The vibrations that have the right symmetry to be Jahn−Teller-active are the e' and the t_2 vibrations. For the doubly degenerate e' vibration, the highest symmetry subgroup is the D_{2d}, so according to the epikernel principle,[41,42] the molecule distorts to that. For the t_2 vibration, the possible symmetries that the molecule can distort to are C_{3v}, C_{2v}, and C_s. We have not scanned the whole potential energy surface of this molecule, but we have checked a few structures, as shown in Tables 1 and 2. Although these geometries have lower energy than the T_d structure of the same multiplicity, they are all much higher than the global minimum singlet D_{4h} structure. The triplet D_{4h} structure is also rather high, ~40−60 kcal/mol higher than the singlet. Therefore, the potential energy surface of this ion seems to have a deep minimum with the D_{4h} singlet structure and then a rather high plateau with a very flat surface with different small local minima on it around the T_d structures. Due to the flatness of this surface, the results may seriously depend on the applied method and level of computation, and this should be a topic for a separate study.

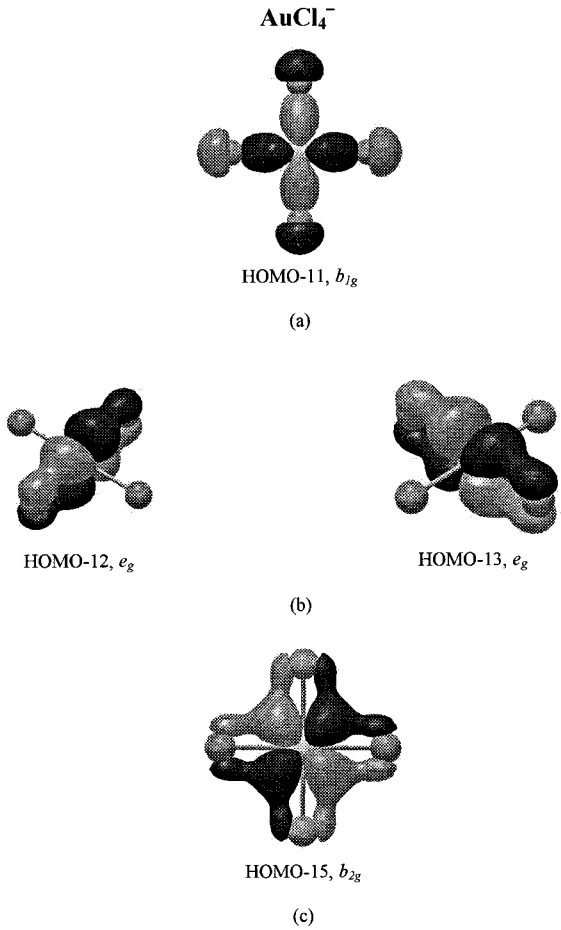

Figure 9. Some of the MOs of the $AuCl_4^-$ ion in square planar (D_{4h}) arrangement. (a) σ MO; (b) out-of-plane π MOs; (c) in-plane π MO (MP2/6-31G(d) for Cl).

Gold Monochloride Monomer and Dimer. Finally, we have also computed the structure of gold monochloride, both its monomer and its dimer. The geometries are given in Table 1. There are two points worth discussing here; one of them is the bond length of the monochloride. While in the gold fluoride analogues the monofluoride bond is ~0.06 Å longer than the shorter bond in AuF_3, in the chlorides, the mono- and trichloride bond lengths are about the same. Generally speaking, we would expect the monohalide bond to be longer than the one in the trihalide, and that happens to be the case for the fluoride but not for the chloride. On the other hand, it was also shown earlier that relativistic effects cause a much larger bond shortening in the monohalides than in the trihalides, 0.16 Å[43] vs 0.05 Å[3] in AuF and AuF_3, respectively. This is due to the fact that only

(40) Akdeniz, Z.; Tosi, M. P. *Z. Naturforsch.* **2000**, *55a*, 495.
(41) Ceulemans, A.; Vanquickenborne, L. G. *Structure and Bonding*; Springer−Verlag: Berlin, 1989; Vol. 71, p 125.
(42) Ceulemans, A.; Beyens, D.; Vanquickenborne, L. G. *J. Am. Chem. Soc.* **1984**, *106*, 5824.

the contraction of the 6s orbitals has to be considered for the monohalides, which is considerable. On the other hand, for the trihalides, the 5d orbitals become part of the valence shell, and their expansion partly compensates for the 6s contraction. The fact that the mono- and trichlorides have about equal bond lengths may indicate that there is a larger amount of covalent character in the trichloride than in the trifluoride, as is also confirmed by Mulliken and NBO analyses.

The other interesting feature of the monochloride is the very short Au···Au distance in the dimer. This has been observed before and is called the aurophilic interaction.[44] It is due to partly relativistic and partly correlation effects. The bond in Au_2Cl_2 is ~0.1 Å longer than in Au_2Cl_6 and the Cl−Au−Cl intra-ring angle in Au_2Cl_2, ~113°, is more than 25° larger than the corresponding angle in Au_2Cl_6 and is unusually large for a four-membered ring. The resulting Au···Au distance is between 2.77 and 2.82 Å, depending on the computational level, and is ~0.7 Å shorter than that in Au_2Cl_6. On the other hand, this gold−gold distance is about the same as, or even shorter than, the same distance in Au_2F_2. The intra-ring orbital interactions in Au_2Cl_2 and Au_2Cl_6 are shown in Figure 8. Although the σ MO of a_g symmetry (Figure 8a,b) is similar in Au_2Cl_2[39a] and Au_2Cl_6,[39b] there is also an additional $d_\pi-d_\pi$ Au···Au interaction in the monohalide dimer,[39c] as can be seen in Figure 8c.

Energies and Populations. The relative energies and dimerization energies are listed in Table 2. The dimerization of $AuCl_3$ is exothermic, similarly to AuF_3, but the energy gain for $AuCl_3$ is smaller, by ~7 kcal/mol, than it is for AuF_3. The calculated BSSE lies in the range of 1−3 kcal/mol per monomer unit at the different B3LYP level computations, but it is rather large, ~6−8 kcal/mol, at the MP2 level calculations. Thus, after correcting for BSSE, the agreement between B3LYP and MP2 computations improves on the dimerization energy.

Investigating the atomic populations (NPA) of the 5d, 6s, and 6p orbitals shows only 5d and 6s participation in bonding for all species considered (Table 6). The Au hybrids are composed of $6s5d^\lambda$ orbitals, with $\lambda > 1$. There is practically no contribution from the 6p orbitals to the bonding. Mulliken populations of all of these species displayed quite significant physically unrealistic negative values for some orbitals. Moreover, in some cases, an "excessive" population [e.g., the +0.065 e of $5d_{xy}$ in $AuCl_4^-$ (Table 6)] was found, which is probably indicative of a general lability floating through the Mulliken populations for this case. As indicated by Weinhold et al.,[22e] natural population is found to give a satisfactory description of ionic species. According to the calculated NBO partial charges of Au, it can be assumed that especially the bonds in the Au(III) species possess a considerably covalent character.

Acknowledgment. We gratefully acknowledge Prof. T. M. Klapötke's (University of Munich) assistance in performing the stabilization of the nozzle system. We thank Prof. Frank Weinhold (University of Wisconsin, Madison) for advice. This work was supported by the Hungarian Scientific Research Fund (Grant No. OTKA T 025788). A.S. thanks the Leibniz Rechenzentrum for a generous allocation of CPU time.

Supporting Information Available: Total electron diffraction experimental intensities at two different camera ranges. This material is available free of charge via the Internet at http://pubs.acs.org.

JA003038K

(43) Schwerdtfeger, P.; Dolg, M.; Schwarz, W. H. E.; Bowmaker, G. A.; Boyd, P. D. W. *J. Chem. Phys.* **1989**, *91*, 1762.

(44) (a) Schmidbaur, H. *Gold Bull.* **1990**, *23*, 11. (b) Pyykko, P.; Runeberg, N.; Mendizabal, F. *Chem. Eur. J.* **1997**, *3*, 1451. (c) Wang, S.-G.; Schwarz, W. H. E. *Angew. Chem., Int. Ed. Engl.* **2000**, *39*, 1757.